

Received October 24, 2018, accepted December 6, 2018, date of publication December 17, 2018, date of current version January 16, 2019.

Digital Object Identifier 10.1109/ACCESS.2018.2887066

# A Review of Biosensors for Non-Invasive Diabetes Monitoring and Screening in Human Exhaled Breath

**FAHAD USMAN**<sup>1,2</sup>, **J. O. DENNIS**<sup>1</sup>, (Senior Member, IEEE), **A. Y. AHMED**<sup>3</sup>, (Member, IEEE), **FABRICE MERIAUDEAU**<sup>4</sup>, (Member, IEEE), **O. B. AYODELE**<sup>5</sup>, **AND ALMUR A. S. RABIH**<sup>6</sup>, (Member, IEEE)

<sup>1</sup>Department of Fundamental and Applied Sciences, Universiti Teknologi PETRONAS, Seri Iskandar 32610, Malaysia

<sup>2</sup>Department of Physics, Al-Qalam University, Katsina PMB 2137, Nigeria

<sup>3</sup>Department of Electrical and Electronic Engineering, Universiti Teknologi PETRONAS, Seri Iskandar 32610, Malaysia

<sup>4</sup>ImViA EA 7535, Team IFTIM Université de Bourgogne, 21000 Dijon, France

<sup>5</sup>International Iberian Nanotechnology Laboratory, 4715-330 Braga, Portugal

<sup>6</sup>Faculty of Engineering and Technology, University of Gezira, Wad Madani 21111, Sudan

Corresponding author: Fahad Usman (fahatu11@gmail.com)

This work was supported by the Universiti Teknologi PETRONAS, Malaysia, through the Graduate Assistant Scheme and the Yayasan Universiti Teknologi PETRONAS-Fundamental Research Grant, Cost Centre, under Grant 015LC0-036.

**ABSTRACT** Exhaled breath acetone has been identified as a diabetes biomarker for non-invasive diagnosis. Its detection using biosensors features has many advantages over the conventional means. This paper reviews the recent literature on the detection of exhaled breath acetone and acetone vapor of diabetic interest. The biosensors have been classified based on their transduction methods. The performance characteristics of the biosensors have been explored for comparison. The future trends are also highlighted.

**INDEX TERMS** Breath acetone, electrochemical biosensors, future trends, mass sensitive sensors, microwave biosensors optical biosensors, operational temperature, relative humidity, sensitivity, transduction.

## I. INTRODUCTION

Diabetes is a chronic disease that occurs either when the pancreas does not produce enough hormone that regulates blood sugar or when the body cannot effectively use the hormone [1]. It can lead to complications in different parts of the body that can result to increase in overall risk of early death. The complication can be heart attack, stroke, kidney failure, leg amputation, vision loss or nerve damage. Furthermore, in pregnancy, poorly controlled diabetes increases the risk of fetal death and other complications. Globally, an estimated 422 million adults were living with diabetes in 2014, compared to 108 million in 1980. According to latest report from WHO, the rising level is still on. In 2014, 8.5% of adults aged 18 years and older had diabetes [2]. In 2015, diabetes was the direct cause of 1.6 million deaths and in 2012 high blood glucose was the cause of another 2.2 million deaths. Forty-three per cent of these deaths occur before the age of 70 years. Early detection and regular screening for diabetes are keys to successful treatment and hindrance of these complications.

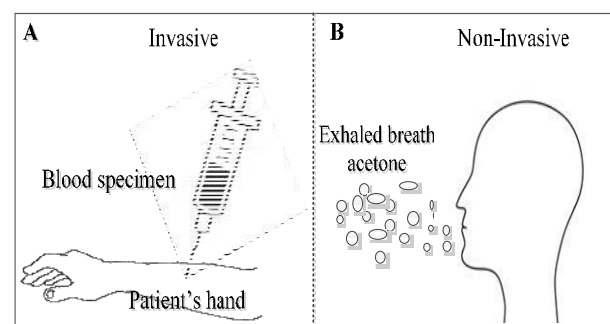


**FIGURE 1. (a) Invasive and (b) Non-invasive sample collection for monitoring and screening of diabetes.**

The usual diagnosis has been through blood glucose level assessment. However, the method features a lot of disadvantages. Few among them are; invasiveness (Figure 1), the need for skilled personnel, time consumption/lack of real time measurement, and laboratory restricted usage [3], [4]. These necessitate investigation of other feasible ways.

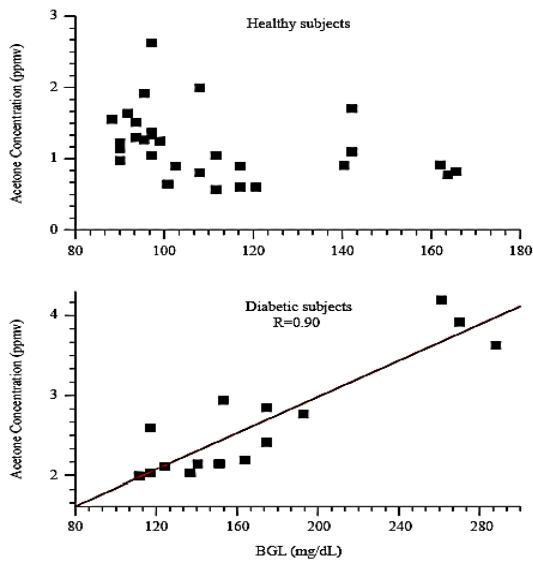


**FIGURE 2.** Correlation between breath acetone and blood glucose (BGL) in healthy and diabetics subjects from Reference [8].

Thousands of volatile organic compounds (VOCs) have been identified in human breath. Interestingly, the VOCs are associated with different human diseases. Exhaled breath acetone has been identified as a biomarker for diabetes [3], [5]–[7] because of its high positive correlation with blood glucose [8] (figure 2). Unfortunately, its concentration in human body is generally very low (0.1 ppm - 0.8 ppm), while it might be high in the case of metabolism disorders, including diabetes mellitus (DM) (1.8 ppm – 5.0 ppm) [7], [9]–[16]. This low concentration has been detected by different devices. The conventional means of acetone detection like gas chromatography–mass spectrometry (GC-MS), selected ion flow tube mass spectrometry (SIFT-MS), proton transfer reaction mass (PTR-MS), high performance liquid chromatography (HPLC), ion mobility spectrometry (IMS), plus laser techniques like tuneable diode laser absorption spectroscopy (TDLAS) and cavity ring down spectroscopy (CRDS) are capable of detecting trace of acetone vapour with better sensitivity and selectivity relatively. However, these methods rely on sophisticated instrumentation, complicated sample collection methods, lack real time measurement, expensiveness and present only at advanced medical institutions [9]–[11].

Biosensors for breath acetone provide lasting solutions to the above mentioned problems [17]–[20].

Biosensors for breath acetone provide lasting solutions to the above mentioned problems [17]–[20]. Most review papers on monitoring and/or screening of diabetes are restricted to either material or exhaled breath acetone based. However, many papers have explored diabetes detection from acetone vapour. Its properties have been assumed to be similar to that of human exhaled breath acetone. Therefore, this paper reviews the latest literatures on the non-invasive

detection of exhaled breath acetone as well as acetone vapour for screening and monitoring of diabetes using biosensors. In addition, papers with lowest detection limit out of diabetes range are excluded. Achievements and challenges have been explained in terms of performance characteristics. Finally, the summary and prospect conclude the review.

## II. BRIEF OVERVIEW OF BIOSENSORS

A biosensor is an analytical device which can detect a biological analyte and convert its response into an electrical signal [19], [20]. Biosensing can also be extended to the detection of any substance or parameter of biological interest. Typical biosensors comprise of three different components [17]. These are: (1) Receptor, which makes the sensing layer. A receptor can be a biological material or any other material that can capture and or interact with the analyte of interest. (2) Transducer, which detects the signal (interaction effect) generated from the interaction. (3) Electronics part, which comprises of amplifiers, processors and display. This helps in translating the information to human understanding.

Many researchers classified biosensor differently. However, in this paper, the biosensors have been classified based on transduction method (figure 3) in accordance with standard sources [20]–[24]. Electrochemical biosensor transforms the electrochemical effect due to analyte-electrode interaction into a useful signal [17], [25]. It could also be due to change in electrical properties from analyte-receptor interaction of any sort. The group comprises of mostly voltammetry (amperometric), potentiometric and chemiresistive sensors.

In optical sensor, a change in optical property due to interaction between analyte of interest and bioreceptor is measured. The usual optical properties exploited are absorbance, reflectance, luminescence, fluorescence, refractive index, optothermal effect and light scattering [17], [23], [25]–[28]. It uses visible and infrared waves. However, in microwave sensors the detection is based on the change of electromagnetic properties of gas sensitive layer (due to acetone sorption) in the microwave range [29]. Resonant characteristics of its system are affected by its design and physical properties of its surrounding environment. Therefore, shifts (due to acetone vapour) observed in their resonant frequencies can be exploited to be used in sensing [30], [31].

Another interesting class of breath acetone biosensor are mass sensitive based devices. They transform the mass change at a specially modified surface into a change of property (frequency) of the supported material. The mass change is caused by accumulation of the analyte of interest. It comprises of mostly piezoelectric, surface acoustic wave and acoustical wave.

For convenience, breath acetone would be referring to both exhaled breath acetone and acetone vapour throughout this paper.

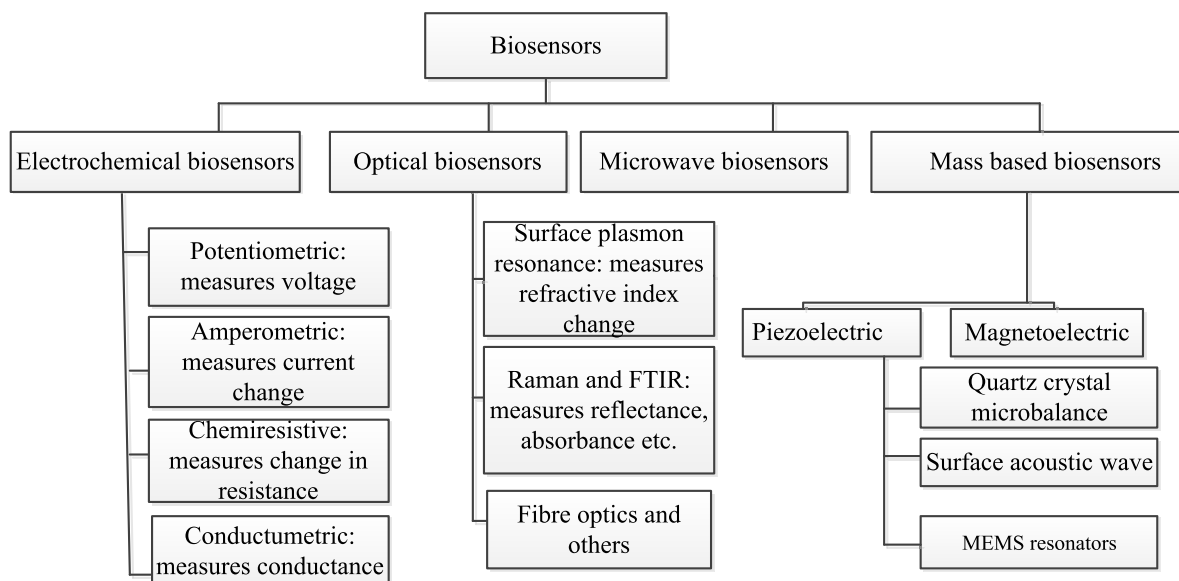


FIGURE 3. Transduction based classification of breath acetone biosensors.

### III. BREATH ACETONE BIOSENSORS FOR MONITORING AND SCREENING OF DIABETES

Ideal breath acetone biosensors for diabetes are required to detect acetone down to sub-part per million (sub-ppm) level [5], [13]. In addition, it must be free or less affected by high relative humidity (RH) [32] as human exhale breath contains about 80% to 90% RH or even more [32]. Furthermore, its user friendliness requires low operation temperature, environmental stability and incorporation of friendly sensing materials [33]–[35].

Many breath acetone biosensors have been tested in laboratories. Despite this achievement, biosensors capable of detecting low concentration of acetone are still lacking commercially. This is likely resulting from the lack of perfection of their performance characteristics. Performance characteristics of usual concern are sensitivity, selectivity, response time, recovery time, limit of detection and stability of the sensing layers [36], [37].

#### A. ELECTROCHEMICAL BREATH ACETONE BIOSENSORS

Over 90% of the tested breath acetone biosensors are chemiresistive/conductometric based. Chemiresistive sensors are explained here under electrochemical biosensors in accordance with [20], [21]. Other explored electrochemical breath acetone biosensors are voltammetry and potentiometric.

A chemiresistor is a resistor whose electric resistance is sensitive to the change in the chemical environment [22], [38]. A chemiresistive sensor consists of one or more electrodes and a detecting layer of the sensor in contact with the electrodes (Figure 4). The measurement of the change in the electrical resistance of the sensing material can be recorded using simple ohmmeter [38]. This generally makes it cheaper and thus, it is relatively widespread. Unfortunately, the performance of chemiresistive sensors is not reliable because of the influence of contact resistance of the electrodes and

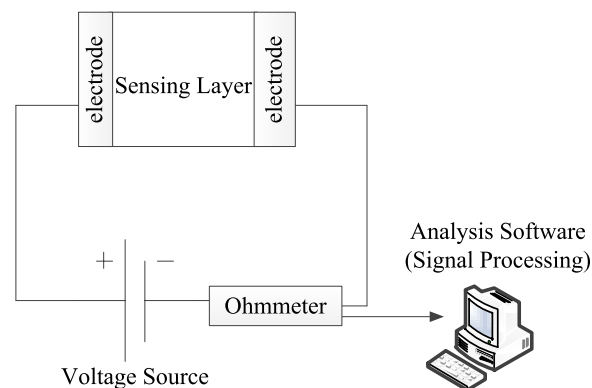


FIGURE 4. A typical chemiresistive sensor.

other ambient factors to the signal. Furthermore, not much information can be obtained other than resistance [38]–[40].

#### 1) SENSITIVITY AND SELECTIVITY IN ELECTROCHEMICAL BREATH ACETONE BIOSENSORS

Sensitivity and selectivity are the basic concern of every biosensor. A lot of efforts have been made toward achieving good sensitivity and selectivity in electrochemical biosensing of breath acetone (for diabetes interest). Selectivity ensures the detection of analyte of interest (breath acetone) in the mix of interfering gases. The popular interfering gases are formaldehyde, trimethylamine and 1,3,5 trimethylbenzene, methanol, acetic acid, Dimethylformamide (DMF), ammonia, pentane (n-C<sub>5</sub>H<sub>12</sub>), toluene (C<sub>6</sub>H<sub>5</sub>CH<sub>3</sub>), carbon monoxide (CO), and ethanol (C<sub>2</sub>H<sub>5</sub>OH) [12], [41]–[45]. Sensitivity also ensures insignificant signal from the interfering gases.

Chemiresistive based breath acetone biosensors for diabetes are compared in table 1. Their active sensing layers are mostly based on metal oxides semiconductors like: Tin(IV) Oxide (SnO<sub>2</sub>), Tungsten (VI) oxide (WO<sub>3</sub>),

**TABLE 1. Chemiresistive based exhaled breath acetone biosensors for diabete.**

| Ref  | Others | ZnO | SnO <sub>2</sub> | WO <sub>3</sub> | Sensing layer  | LOD (ppm) | Response (%)         | Recovery/Response Time (s) | O.T. (°C)/ R.H. (%) |
|------|--------|-----|------------------|-----------------|--|-----------|----------------------|----------------------------|---------------------|
| [71] |        | x   |                  |                 | Three-dimensional ordered ZnO-CuO  | 0.1       | 1.8                  | 1.4/2.4                    | 310/ 94.5           |
| [46] |        |     | x                |                 | Carbon nanotubes-SnO <sub>2</sub> nanocomposite  | 0.5       | 100                  | N.M./ N.M.                 | 200/85              |
| [41] |        |     | x                | x               | Indium loaded WO <sub>3</sub> /SnO <sub>2</sub> nanohybrid   | 1         | 4.4@1ppm             | 2/4                        | 200/N.M.            |
| [33] | x      |     |                  |                 | Monolayer graphene   | 0.3       | (1)1.89              | N.M./ N.M.                 | R.T./N.M.           |
| [62] | x      |     |                  |                 | Non stabilized zirconia and NiNb <sub>2</sub> O <sub>6</sub>   | 0.5       | -1.4mv/decade@500ppb | <10                        | 650/92.7            |
| [81] |        | x   |                  |                 | 3D-ordered ZnO-Fe <sub>3</sub> O <sub>4</sub> inverse opal   | 0.1       | 2.8                  | Small                      | 485/N.M.            |
| [64] | x      |     |                  |                 | Single-crystalline Fe <sub>2</sub> O <sub>3</sub> mesoporous nanospheres   | 0.1       | 16                   | 50/2                       | 170/93.6            |
| [83] |        | x   |                  |                 | NiO/ZnO hollow spheres   | 0.8       | 30@100ppm            | 20/1                       | 275/N.M             |
| [32] |        |     |                  | x               | Si:WO <sub>3</sub>   | 0.02      | N.M.                 | 35-70/10-15                | /80-90              |
| [51] |        |     |                  | x               | γ-Fe <sub>2</sub> O <sub>3</sub> :WO <sub>3</sub> nanocomposite  | 1         | 3.93                 | 3/1                        | 300/N.M             |
| [52] |        |     | x                |                 | SnO <sub>2</sub> -MWCNT nanocomposites   |           | N.M.                 | N.M./ N.M.                 | 350/N.M             |
| [65] | x      |     |                  |                 | Monolayer graphene   | 0.1       | 0.4                  | 300 /300                   | /N.M                |
| [66] | x      |     |                  |                 | Zirconia and Co1-xZnxFe <sub>2</sub> O <sub>4</sub>  | 0.3       | 132mv/decade@100ppm  | N.M. N.M.                  | 650/98              |
| [67] | x      |     |                  |                 | In <sub>2</sub> O <sub>3</sub> hollow nanofibers   | 0.02      | 151@5ppm             | N.M./ N.M.                 | 300/N.M             |
| [12] |        |     | x                |                 | Eu-doped SnO <sub>2</sub> electrospun nanofibers   | 0.3       | 32.2@100ppm          | 3/4                        | 280/N.M             |
| [68] | x      |     |                  |                 | (Au NPs)-modified α-Fe <sub>2</sub> O <sub>3</sub> columnar superstructures (Au/α-Fe <sub>2</sub> O <sub>3</sub> CSS)                      | ppb range | 42                   | 16/13                      | 150/N.M             |
| [69] | x      |     |                  |                 | Pt-decorated In <sub>2</sub> O <sub>3</sub> nanoparticles  | 1         | 12@1ppm              | 90/15                      | 200/75              |
| [84] | x      |     |                  |                 | Pt@In <sub>2</sub> O <sub>3</sub> core-shell nanowires   | 0.01      | 6.23 @ 1 ppm         | 13/11                      | 320 /100            |
| [43] |        |     |                  | x               | cuboid WO <sub>3</sub> nanosheets  | 0.5       | 49.1@100ppm          | 19/7                       | 300 &340/N.M.       |
| [85] |        |     |                  | x               | α-Ag <sub>2</sub> WO <sub>4</sub> nanorods   | 0.5       | 2.1@2ppm             | 46/30                      | 350/N.M.            |
| [78] | x      |     |                  |                 | palladium doped LaFeO <sub>3</sub>   | 1         | N.M. 2.1 @1ppm       | 2/4                        | 200/N.M.            |
| [72] | x      |     |                  |                 | Pure and Pt-loaded gamma iron oxide  | N.M.      | 65%@1ppm             | 315/14                     | 250/N.M.            |
| [60] |        | x   |                  |                 | Maize straw-like ZnO:Ni  | 0.116     | 68@100ppm            | 2/6                        | 340/95              |
| [58] |        |     |                  | x               | WO <sub>3</sub> nanofibers functionalized by Rh <sub>2</sub> O <sub>3</sub> nanoparticles  | N.M.      | 41@5ppm              | 434.09/110.69              | 350/90              |
| [50] |        |     |                  | x               | Porous WO <sub>3</sub> nanofibers  | 0.1       | 60.2 @100ppm         | 4-9/6-13                   | 270/95              |
| [34] |        |     |                  | x               | Tungsten trioxide-polyaniline nanocomposites   | 10        | N.M.                 | N.M./ N.M.                 | R.T./N.M.           |
| [55] |        |     |                  | x               | Co-doped WO <sub>3</sub> hierarchical flower-like nanostructures   | N.M.      | 103 @100ppm          | 10/2                       | 350/N.M             |
| [73] | x      |     |                  |                 | Nano-titania thin film   | 0.5       | 115                  | 22/14                      | 150/N.M             |
| [61] |        | x   |                  |                 | Nanostructured Cerium-doped ZnO thin film  | 1         | 3@5ppm               | N.M./ N.M.                 | 24/N.M              |
| [86] |        | x   |                  |                 | Catalyst Loaded ZnO/ZnCo <sub>2</sub> O <sub>4</sub>   | 0.4       | 69                   | N.M./ N.M                  | 250/90              |
| [74] | x      |     |                  |                 | Stabilized zirconia and CdMoO <sub>4</sub> sensing electrode   | N.M.      | -133.5(mv)@100ppm    | N.M./ N.M.                 | 625/N.M             |
| [75] | x      |     |                  |                 | Ytterbium ferrites nanocrystalline powders   | 0.1       | 1.72                 | N.M./ N.M.                 | 230/N.M             |
| [53] |        |     | x                |                 | Samarium oxide loaded tin oxide (Sm <sub>2</sub> O <sub>3</sub> /SnO <sub>2</sub> )  | 0.1       | 41.14                | N.M./ N.M                  | 250/ N.M.           |
| [54] |        |     | x                |                 | Hollow Pt-Functionalized SnO <sub>2</sub> Hemipill Network   | 0.0036    | N.M                  | 72 s / 120s                | 300/80              |
| [44] |        |     |                  | x               | Porous C-doped WO <sub>3</sub> hollow spheres by carbon spheres  | 0.2       | 1.8 @0.9ppm          | N.M./ N.M.                 | 300/90              |
| [35] | x      |     |                  |                 | Nanostructured K <sub>2</sub> W <sub>7</sub> O <sub>22</sub>   | 1.2       | N.M                  | N.M./12                    | R.T./N.M.           |
| [45] |        |     |                  | x               | PPy-WO <sub>3</sub> Hybrid Nanocomposite   | N.M.      | N.M                  | N.M./ N.M.                 | 90/N.M              |
| [87] | x      |     |                  |                 | Pt-loaded -Fe <sub>2</sub> O <sub>3</sub> porous nanospheres   | 0.8       | 27.2                 | N.M./1s                    | 220/ N.M.           |
| [49] | x      |     |                  |                 | Chitosan   | 0.1       | 3.9@0.1 ppm          | <200/10                    | 25-30/N.M.          |
| [5]  | x      |     |                  |                 | 3-D TiO <sub>2</sub> Nanoflowers   | 1         | 3.45@1ppm            | 15-39/6-15                 | 60/75               |
| [29] |        |     |                  | x               | Hierarchical WO <sub>3</sub> core-shell microspheres   | 1.8       | N.M                  | N.M./9.8                   | 350/N.M.            |
| [59] |        |     |                  | x               | Si-Doped WO <sub>3</sub> Thin Films  | 0.32      | 15.8@0.32ppm         | 150 s/60 s                 | 425/50              |
| [57] |        |     | x                |                 | Eu-doped SnO <sub>2</sub>  | 0.3       | 32.2@100ppm          | 3/4                        | 280/N.M.            |
| [47] | x      |     |                  |                 | Self-assembly of monolayer-capped gold nanoparticles   | N.M.      | N.M                  | N.M./ N.M.                 | /N.M.               |
| [63] | x      |     |                  |                 | TiO <sub>2</sub> nanoparticles functionalized In <sub>2</sub> O <sub>3</sub> nanowires (In <sub>2</sub> O <sub>3</sub> /TiO <sub>2</sub> ) | 0.1       | 33.34@10ppm          | 131.28/ 62.86              | 250/N.M.            |
| [77] | x      |     |                  |                 | W-doped NiO hierarchical nanostructure   | N.M.      | 198.1 to 100 ppm     | N.M./ N.M.                 | 250/                |
| [76] |        |     | x                |                 | C <sub>3</sub> N <sub>4</sub> -tin oxide   | 0.067     | 11@20ppm             | 8/7                        | 380/35-45           |
| [88] | x      |     |                  |                 | Ytria- stabilized zirconia (YSZ) and columbite composite oxide   | 0.2       | -25 mV to 5 ppm      | 21/9 @2ppm                 | 600/98              |
| [42] |        |     |                  | x               | C-doped WO <sub>3</sub>  | 0.2       | 1.8 @ 0.9 ppm        | 6-12 /3-9                  | 300/95              |
| [56] |        |     |                  | x               | WO <sub>3</sub> nanocrystals   | 0.05      | 3.37@0.9ppm          | < 30/< 30                  | 300/N.M.            |

Copper (II) oxide (CuO), Zinc oxide (ZnO), Titanium dioxide (TiO<sub>2</sub>), Indium (III) oxide (In<sub>2</sub>O<sub>3</sub>), and Iron (III) oxide (Fe<sub>2</sub>O<sub>3</sub>) [43]. In addition, some are based on other chemiresistive materials like: graphene [33], carbon nanotubes [46], nanoparticles [47] and conducting polymers [48], [49]. Furthermore, the materials are mostly either in their real form [42], [50] or in composite [45], [51].

*a: IMPROVEMENT OF SENSITIVITY AND SELECTIVITY IN DIFFERENT CHEMIREISTIVE BASED MATERIALS*  
*i) TIN(IV) OXIDE BASED CHEMIREISTIVE BREATH ACETONE BIOSENSORS*

Modifications to various novel materials based on SnO<sub>2</sub> (either in pure form or composite) provide good sensitivity and selectivity to breath acetone [12], [41], [46], [52].

For example, [41] has proved good sensitivity and selectivity of indium loaded  $\text{WO}_3/\text{SnO}_2$  nanohybrid ( $\text{In}/\text{WO}_3\text{-SnO}_2$ ) based biosensor. Comparison has been made among interfering VOCs like ethanol, formaldehyde, trimethylamine and 1,3,5 trimethyl benzene. It also shows improved response compared to  $\text{WO}_3/\text{SnO}_2$  based biosensor. The short response/recovery times of the sensor proved its potentiality in real time measurement.

The response of pure  $\text{SnO}_2$  has also been increased by more than 2.29 times after loading samarium oxide ( $\text{Sm}_2\text{O}_3$ ) [53]. The lowest detection limit (LOD) was as low as 100 ppb. This has been attributed to increase in oxygen vacancies created by the substitution of samarium in the  $\text{SnO}_2$  lattice.

Functionalization of  $\text{SnO}_2$  hemipill network with a hollow Pt has shown a superior detecting capability toward acetone over non-functionalized one [54]. It has detected 200 ppb of acetone under high humidity (RH 80%) with LOD down to 3.6 ppb.

Inclusion of carbon nanotubes to metal oxides semiconductors has also improved the sensitivity and selectivity in the breathe acetone detection [46]. For example, carbon nanotube- $\text{SnO}_2$  nanocomposite showed good selectivity to breath acetone after a comparison with ethanol. In addition, the sensitivity of the sensor was improved down to the detection limit of about 0.5 ppm [46].

Multiwall carbon nanotubes (MWCNT) composite also showed an increment in response from 50% to 80% due to loading of MWCNT in  $\text{SnO}_2$ -MWCNT nanocomposites based breath acetone sensor [52]. The sensor's stability is more than one year.

In another work, a lanthanide series element, particularly Europium (Eu) has been added to  $\text{SnO}_2$  with the aim to increase the sensitivity and selectivity. Reference [12] has compared pure  $\text{SnO}_2$  nanofibers with Eu-doped  $\text{SnO}_2$  nanofibers based breath acetone sensors. Eu-doped  $\text{SnO}_2$  electrospun nanofiber sensor shows better breath acetone selectivity and sensitivity among ethanol, methanol, acetic acid, DMF and ammonia.

#### *ii) $\text{WO}_3$ BASED CHEMIREISTIVE BREATH ACETONE BIOSENSORS*

$\text{WO}_3$  has also attracted attention due to its promising physical and chemical properties. Its sensing characteristics can be enhanced with doping. A biosensor based on Si-doped epsilon- $\text{WO}_3$  nanostructured films has been developed [32]. It proves a low detection limit of acetone ( $\sim 20$  ppb) with short response (10–15 s) and recovery times (35–70 s [32]).

Morphological changes in the Co-doped  $\text{WO}_3$  hierarchical flower-like nanostructures assembled with nanoplates (FNPs) as well as its defect of  $\text{WO}_3$  lattice and Co-catalysis effect have also promoted breath acetone adsorption [55].

In another development, n-n heterojunction in the  $\gamma\text{-Fe}_2\text{O}_3:\text{WO}_3$  nanocomposite based biosensor improved the detection of breath acetone. Improved response down to 1 ppm has been observed as against pure  $\text{WO}_3$  and pure  $\gamma\text{-Fe}_2\text{O}_3$  alone. Its selectivity to breath acetone with a very

fast response (1s) and very short recovery time (3s) against alcohol vapour and moisture in human breath has been proved [51].

Another group of researchers used thickness-controlled cuboid  $\text{WO}_3$  Nano sheets based biosensor to prove the good sensitivity and selectivity to acetone vapour against ethanol [43].

Furthermore, the sensing layer of its nanocrystal form ( $\text{WO}_3$  nanocrystals) was able to attain a detection limit down to 0.05 ppm [56].

The synthesis of hierarchical  $\text{WO}_3$  core-shell microspheres also allowed the detection of acetone vapour down to 1.8 ppm. The sensing layer has also shown to possess better response to breath acetone compared to ethanol, methanol,  $\text{NH}_3$ , Xylene and Toluene [57].

Porosity of the biosensor layer ( $\text{WO}_3$ ) has also helped in attaining selective and sensitive breath acetone detection. It demonstrated good response and selectivity down to 0.1ppm compared to ethanol, toluene, methanol, benzene,  $\text{NH}_3$  and CO. Porous C-doped  $\text{WO}_3$  hollow spheres based biosensor is also very sensitive and selective to breath acetone down to 0.2 ppm [44]. The research was the improvement of the previous work done by the same researchers [42].

Another important factor is the catalytic sensitization of the sensing layers [50]. Highly sensitive and selective breath acetone detection has been achieved following the functionalization of  $\text{WO}_3$  nanofibers (NFs) by Rhodium nanoparticles ( $\text{Rh}_2\text{O}_3\text{NPs}$ ) [58]. This was proven against interfering gases like pentane ( $\text{n-C}_5\text{H}_{12}$ ), ammonia ( $\text{NH}_3$ ), toluene ( $\text{C}_6\text{H}_5\text{CH}_3$ ), carbon monoxide (CO), and ethanol ( $\text{C}_2\text{H}_5\text{OH}$ ) [58].

The unique properties of conducting polymers attracted the synthesis of polypyrrol (PPy)- $\text{WO}_3$  Hybrid Nanocomposite. The composite showed better selectivity and sensitivity to breath acetone while compared to ethanol, methanol and water [45].

Doping of tungsten oxide film with Si significantly improved the limit of detection of breath acetone down to 0.32 ppm compared with the pure  $\text{WO}_3$  [59]. Effect of relative humidity has also been explored at 50%.

#### *iii) ZnO BASED CHEMIREISTIVE BREATH ACETONE BIOSENSORS*

Another great metal oxide semiconductor for breath acetone biosensing is Zinc Oxide (ZnO). ZnO thin films show promising features in the detection of breath acetone for diabetes interest [12]. It showed good sensitivity and better selectivity to acetone compared to ethanol and acetaldehyde.

A biosensing layer based on maize straw-templated hierarchical porous Ni doped ZnO (STHPS  $\text{ZnO}:\text{Ni}$ ) has been synthesized [60]. Its ability to provide real time measurement of breath acetone was proven from its short response (6s) and recovery times (2s). Its detection limit was estimated as 116 ppb.

ZnO based biosensor can also be improved with doping. Thin films of Nanostructured Cerium doped ZnO have also

been synthesised [61]. Greater response to acetone vapour against ammonia and acetaldehyde vapours has indicated their selective nature.

#### *iv) OTHER CHEMIREISTIVE BREATH ACETONE BIOSENSORS*

Different other materials (other than  $\text{SnO}_2$ ,  $\text{WO}_3$  and  $\text{ZnO}$ ) have also been explored [5], [33], [35], [49], [52], [62]–[77]. Table 1 shows details about all the chemiresistive sensors for diabetes. Most of their LOD covers diabetes range. However, few start from range of doubt [5], [35], [78]. Range of doubt means the range between normal and diabetes (which indicates those at risk).

#### *b) IMPROVEMENT OF SENSITIVITY AND SELECTIVITY IN OTHER ELECTROCHEMICAL BREATH ACETONE BIOSENSORS*

Potentiometric biosensors are very promising acetone detectors. The principle of detection is based on the measurement of the emf (electrical potential) of a cell at zero current (during exposure to breath acetone). The emf is then proportional to the logarithm of the concentration of the breath acetone. For example, a Light Addressable Potentiometric Sensors (LAPS) has been used in the detection of breath acetone for diabetes [79]. Also, another sensitive breath acetone sensor has been developed based on immobilised  $\alpha$  D- galactose [80]. Its potentiometry used three electrodes, a working electrode (made of platinum), reference electrode (silver/silver chloride/0.3M KCl) and counter electrode (copper). A portable gas analyzing system has also been developed using polypyrrole (ppy) conducting polymer sensor [48]. The detection of the acetone was translated from voltage variation rate. They were able to validate their results using samples from normal subjects and diabetics.

## 2) OPERATION TEMPERATURE

Operational temperature is another important parameter in biosensing application. Despite the promising sensitivity and selectivity of these electrochemical biosensors, high operational temperature has always been their main shortcoming as shown in table 1 [62], [66], [74], [81]. High operational temperature is prone to problems like greater power consumption, reduced device lifetime, unfeasible accommodation of inflammable substances and other environmental effects. A lot of efforts have been conducted in a move to suppress such high operation temperature ( $200^\circ\text{C}$  to  $600^\circ\text{C}$ ) to room temperature or lower (Table 1).

Conducting polymers are well researched in biosensing field. This is due to their attainable high sensitivity, short response time, room temperature operation and many more. Tungsten trioxide-polyaniline nanocomposite has allowed room temperature detection of acetone vapour as against normal Tungsten trioxide ( $\text{WO}_3$ ) with temperature of almost  $\geq 300^\circ\text{C}$  [34]. Unfortunately, the LOD (10ppm) was only closer to diabetes range. But, Chitosan-based biosensor has allowed the detection of low concentration acetone at the temperature of ( $\sim 25$ – $30^\circ\text{C}$ ) in normal air [49].

A Nanostructured Cerium-doped  $\text{ZnO}$  thin film based breath acetone sensor has detected breath acetone down to 1ppm at  $24^\circ\text{C}$ . Its response was also within acceptable range (3% at 5ppm) [61]. Also, another nanostructure, nanostructured  $\text{K}_2\text{W}_7\text{O}_{22}$  based breath acetone has also provided room temperature operation with good response time. This was attributed to its unique ferroelectric and semiconducting properties that result in the effective interaction and strong charge transfer between acetone and  $\text{K}_2\text{W}_7\text{O}_{22}$  [35]. Its LOD was also within the required range for the screening and monitoring of diabetes.

Hierarchical 3-D  $\text{TiO}_2$  Nanoflowers also gave rise to a highly selective low-temperature ( $60^\circ\text{C}$ ) acetone sensor [5]. The selectivity was judged among methanol, 2-butanone, toluene, and 2-propanol. Its ability to provide real time measurement has been observed from its fast response ( $\sim -15$  s) and recovery time ( $\sim 15$ – $39$  s). Reference [82] were also able to investigate how a  $\text{ZnO}$  thin film prepared by sole gel dip coating can be used as a breath acetone biosensor at room temperature. Recently, another conducting polymer-metal oxide composite (PPy- $\text{WO}_3$  hybrid nanocomposite) based gas sensor deposited by electrospinning has also provided a selective and sensitive detection of breath acetone at low temperature ( $90^\circ\text{C}$ ). The enhancement in the detection by the PPy- $\text{WO}_3$  hybrid nanocomposite film was attributed to the effective role of  $\text{WO}_3$  nanoparticles in PPy matrix and formation of p-n heterojunction region [45]. The latest work on the effect of ultraviolet illumination on monolayer graphene-based resistive sensor showed the capability of detecting acetone at room temperature. The unique effect could even provide the detection down to ppb range. The improvement of operational temperature could open a way to achieving feasible electrochemical breath acetone biosensors for monitoring and screening of diabetes.

## 3) RELATIVE HUMIDITY

An environmental condition like relative humidity (RH) influences the performance of biosensors. Thus, a reliable biosensor layer is always expected to be characterised with water-vapour resistant feature [89], [90]. Additionally, breath acetone is highly humidified (80-90% R.H.). As such, reliable detection of acetone requires insensitivity to relative humidity or moisture.

Many researchers investigated the effect of relative humidity on the response of their exhaled breath acetone biosensors as shown in table. Only few biosensors were optimised at such high humidity. For example, [48] showed insignificant R.H. effect to their Polypyrrole based biosensor. Unfortunately, the maximum explored relative humidity effect was 45%. In another development, a portable Si (silicon): $\text{WO}_3$  based breath acetone sensor has shown the cross sensitivity to humidity to decreased considerably to 4.5% between 80 and 90% R.H. [32]. The effect of competition between acetone and water adsorption has been explored on Carbon nanotubes- $\text{SnO}_2$  nanocomposite based biosensor at 85% RH (RH of human breath at  $37^\circ\text{C}$ ) [46]. Though its

response has been decreased, but it was within acceptable level.

As a rule, breath acetone sensors need to be optimised for R.H. (at around 80-98%) [32], [44], [46], [50], [58], [60], [62], [64]–[66], [71]. The response of sensors usually decreases with increase in the concentration of moisture (RH increase). This might be due to the displacement of chemisorbed oxygen species by water molecules and hydroxyl species at the sensor surface. However, even with the decrease, response values used to be within acceptable range. In a move to manage this decrease, a WO<sub>3</sub> nanofibers (WO<sub>3</sub>NFs) biosensor film has been decorated with Rh<sub>2</sub>O<sub>3</sub>. Maintenance of remarkable sensing properties has been observed even in 95% RH at room temperature (28°C) [58].

Addition of 0.25% MWCNT to pristine SnO<sub>2</sub> to form composite biosensor also showed insensitivity to saturated moisture [52]. Hence, reliability of any breath acetone biosensor cannot be proven without RH optimization.

## B. OPTICAL BREATH ACETONE BIOSENSORS

An optical biosensor is a device that can measure a change in an optical property due to molecular binding or reactions and converts it into an electrical signal [23], [37]. Optical based biosensors are recommended over other biosensors because their unique advantages such as greater sensitivity, electrical passiveness, freedom from electromagnetic interference, wide dynamic range, non-requirement of reference electrode, freedom from electrical hazards, high stability relatively, potential for higher-information content than electrical transducers and multiplexing capabilities. Despite all these advantages, only few breath acetone sensors were explored based this transduction method [29], [91]–[97].

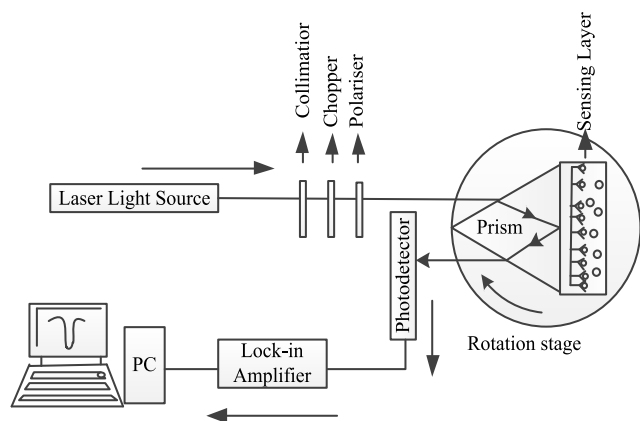


FIGURE 5. A typical Surface Plasmon Resonance (SPR) sensor.

### 1) SENSITIVITY AND SELECTIVITY

As described earlier, only few researchers explored optical detection of breath acetone for diabetes. These works were mostly based on fiber optics, spectroscopic and surface plasmon resonance methods. Figure 5 shows sketch of an optical sensor based on surface plasmon resonance.

A fiber optic nicotinamide adenine dinucleotide (NADH) measurement system has provided a very selective and sensitive detection of breath acetone down to 20 ppb (applicable in monitoring diabetes) [91]. Photomultiplier tube (PMT) photodetector monitors the change of fluorescent emitted from NADH following the detection of acetone vapour.

In another development, a highly selective portable optical acetone sensor was achieved by monitoring the absorbance in Flavan, a product from reaction of acetone and resorcinol on Nafion (a perfluorosulfonic acid polymer membrane). The Flavan produces a color change in the visible spectrum which could measure acetone concentrations to less than a ppm [92].

Raman spectroscopy was also used in the detection of acetone vapour will LOD down to 0.0037 ng (ppb range) [93]. The sensor signal was extracted from the enhanced Raman signal following the adsorption of the acetone vapour at the tips of the nano-pillar substrates.

A portable sample preconcentration and cavity enhanced spectroscopy based biosensor has demonstrated the measurement of 159 ppbv concentration of breath acetone [94].

Acetone vapour detection (in diabetes range) has also been achieved with surface plasmon resonance based biosensor [95]. The biosensor has shown better selectivity to acetone vapour against methanol, ethanol and propanol. A facile microwave irradiation of porous Au-decorated 1D  $\alpha$ -Fe<sub>2</sub>O<sub>3</sub> has achieved ultrahigh-sensitivity in acetone detection [96]. The sensor exhibits a close to linear response and fast dynamics in response/recovery cycling over a wide range of acetone concentration (–100 ppm range in humid air).

A polymer-coated microring resonator has been explored for breath acetone sensing [98]. The authors used two low molecular weight polymers, hybrane D2800 and PVP-NH<sub>2</sub> as gas absorption materials for the sensor. Experimental and theoretical LOD for acetone of 100 ppb and 17 ppb were obtained, respectively.

Also, a highly sensitive breath acetone biosensor has been tested based on silicon nanophotonic ring resonator [99]. A sensitivity of 1.7 peak shift / 1000 ppm was recorded for breath acetone detection with high stability (<1pm drift) and fast response time (~20 s). However, the achieved detection limit (800 ppm) is not applicable to the monitoring of diabetes.

Recently, an LOD down to 0.5 ppm has been achieved by a modified sodium alginate gel fabricated filter paper based sensor [100].

### 2) OPERATION TEMPERATURE

The effect high temperature might not be an issue with optical sensor. Most the optical based biosensors mentioned above provided the result of their measurement at feasible temperature range [100]. However, Au/1D  $\alpha$ -Fe<sub>2</sub>O<sub>3</sub> based biosensor was the only sensor reported to have been operated at 270°C [96]. Therefore, more comprehensive studies are still encouraged in this regard.

3) RELATIVE HUMIDITY

The effect of relative humidity was also not studied in most of the available literature. For example, all the reported literature [91]–[97] on the optical detections fail to present any RH studies. Therefore, future studies are also expected to look into it.

C. MICROWAVE BREATH ACETONE BIOSENSORS

Microwave-based sensors have shown huge potential in sensing applications [29], [101]. They can provide a non-contact and real time measurement. This makes them more attractive for sensing application [102]. Schematic diagram of the sensor used by [103] is illustrated in Figure 6.

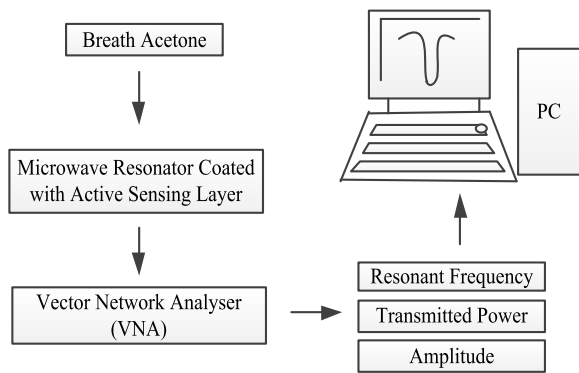


FIGURE 6. A schematic diagram of a microwave detection of breath acetone using microwave resonator.

Recently, microwave based detection of breath acetone has been explored by some researchers. For example, a room temperature (37°C) detection of breath acetone has been achieved down to 1 ppm [104]. The authors attributed the success to the unique features of microwave sensors, large surface area of the sensing layer (Highly Networked Capsular Silica Porphyrin Hybrid Nanostructures) and its numerous active sites. Also, another room temperature detection has been achieved by [29]. Its measurement was based on comb polymer phthalocyanines (Pc)-thin film deposited on interdigital capacitor. Unfortunately, the LOD achieved was 0.5 ppm. Therefore, it needs to be improved to cover the entire range for both healthy and diabetes patients. Detection of low concentration of acetone (0–265 ppt) has been conducted [103]. The measurement was based on the absorption of acetone by a microwave resonator coated with a thin layer of polydimethylsiloxane (PDMS). Many studies are still required in this promising area.

D. MASS SENSITIVE BREATHE ACETONE BIOSENSORS

Mass sensitive based biosensors are very generally sensitive to mass change. They transform the mass change at a specially modified surface into a change of a property of the support material [105]. The mass change is caused by the accumulation of the analyte of interest (mass loading). The signals are mostly extracted based on frequency shift. Figure 7 illustrates a breath acetone sensor based on

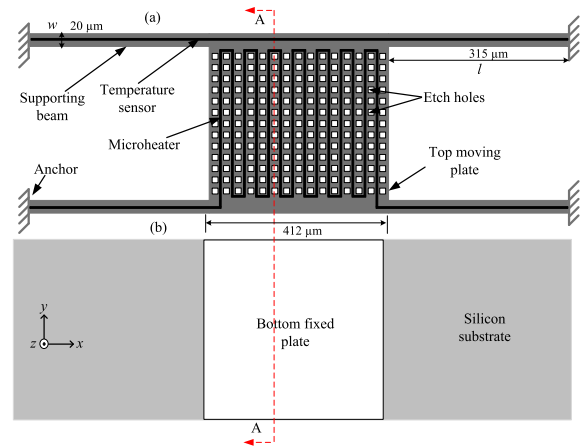


FIGURE 7. Schematic diagram of a polyMEMS breathe acetone biosensor utilising mass sensitivity effect; (a) moving plate and (b) the bottom fixed plate [106].

MEMS resonator [106]. It was made of a square moving plate supported by four flexible beams, and suspended on top of a fixed plate with an initial gap.

Many researchers have investigated the detection of acetone using piezoelectric quartz crystal microbalance (QCM) concept. However, most of the studies are irrelevant to this review [107]–[119]. A quartz crystal microbalance sensor utilizing Ag<sup>+</sup>-ZSM-5 zeolite as an active element was found to be highly sensitive to acetone with detection limit down to 1.2 ppm. But, it was reversible only in nitrogen [120]. Piezoelectric sensing is based on the measurement of the frequency change of the quartz oscillator plate caused by adsorption of a mass of the analyte at the oscillator. When a voltage is applied to a quartz crystal, it oscillates at a specific frequency. Change in mass on the quartz surface is related to the change in frequency of the oscillating crystal, as shown by the Sauerbrey equation [121].

$$\Delta m = -C \cdot \Delta f$$

QCM can work at room temperature as a mass sensitive sensor and can determine even nanogram-level mass change [122]. Graphene oxide/chitosan (GO/CS) nanocomposite based QCM sensor has been used in the detection of some amine vapours. A mass sensitive Complementary-Metal-Oxide-Semiconductor Micro-Electro-Mechanical Systems (CMOS-MEMS) based breath acetone biosensor with detection limit down to 0.4 ppm has also been simulated at room temperature [123]. It was experimentally tested for concentration of breath acetone down to 0.05 ppm using a polyMEMS device [124]. In another development, the possibility of intergrating hierarchical ZnO nanostructure to CMOS-MEMS has been described [125]. This promising high sensitivity of mass sensitive based biosensors is expected to allow the detection of breath acetone for monitoring and screening of diabetes in near future. Recently, 1 butyl-3-methylimidazolium tetrafluoroborate ([bmim][BF<sub>4</sub>]) has been coated on a quartz crystal microbalance (QCM) for the detection of breath acetone for diabetes monitoring.



The sensing mechanism was based on a reduction in viscosity and density of the [bmim][BF<sub>4</sub>] film. The recorded sensitivity and LOD were 3.49 Hz/ppmv and 5.0 ppmv, respectively. Therefore, future studies are expected to take this area to maturity for reliable and improved monitoring and screening of diabetes.

#### IV. CONCLUSIONS AND FUTURE TRENDS

Breath acetone has been well validated as diabetes biomarker that can provide a non-invasive means of monitoring and screening diabetes. Since then, researchers have been looking for novel ways to allow its detection at very feasible and favourable condition. The utilisation of biosensor for breath acetone detection features many advantages over the conventional means of its detection (using gas chromatography– mass spectrometry (GC-MS), selected ion flow tube mass spectrometry (SIFT-MS), proton transfer reaction mass (PTR-MS), high performance liquid chromatography (HPLC)). Biosensors provide real time measurement. In addition, it is portable, cheap and easily operated and accessible.

Electrochemical biosensors, particularly chemiresistive biosensors have been used widely in the detection of breath acetone for the monitoring and screening of diabetes (5ppm downward). This might have resulted from the simplicity of the detection system. However, chemiresistive biosensors are generally regarded as extremely unselective sensors due to the resistance influence from the component of the detection system. But, researchers had made a lot of contributions toward improving the biosensors. Their selectivity test was usually against interfering gases like formaldehyde, trimethylamine and 1,3,5 trimethylbenzene, methanol, acetic acid, DMF, ammonia, pentane, toluene, carbon monoxide, ethanol. Unfortunately, most of these chemiresistive breath acetone sensors use metal oxide semiconductors which are well known to be operated at very high temperatures (300°C to 650°C). These pose problems to the biosensors, users and the environment. Additionally, the effect of relative humidity on biosensing layer needs closer consideration since exhaled breath acetone is greatly rich in moisture (80-95% RH). It reduces the response of the biosensors [3], [46], [56]. Researchers find hindering the effect of RH very difficult. But, its minimization to acceptable level has been achieved by many researchers.

In the same vein, optical, microwave and mass sensitive based biosensors might be very promising in the detection of breath acetone for diabetes due to their unique properties and better sensitivity. More importantly, are the improved selectivity, electrical passiveness, freedom from electromagnetic interference, wide dynamic range of operation, non-requirement of reference electrode, freedom from electrical hazards of the optical based sensors. Unfortunately, optical based breath acetone sensing is not even close to maturity. In the case of promising mass sensitive based biosensors, a lot of efforts have been made. However, our search had only located few papers that has been optimised for the

detection breath acetone for monitoring and screening of diabetes [120]. Microwave based biosensors also lack popularity in the detection of breath acetone for diabetes.

Conclusively, chemiresistive sensors still seem to be the most sensitive breath acetone biosensors. However, their detection system, selectivity and high operational temperature still need improvement. As for the other biosensors where low operational temperature and good selectivity are mostly achieved, vigorous studies are still expected in order to improve their sensitivity. Addressing these issues would definitely improve and open a way to achieving a reliable biosensor for non-invasive monitoring and screening of diabetes.

#### REFERENCES

- [1] *NMH Fact Sheet February 2010-Diabetes*. Accessed: Feb. 12, 2018. [Online]. Available: [http://www.who.int/nmh/publications/fact\\_sheet\\_diabetes\\_en.pdf](http://www.who.int/nmh/publications/fact_sheet_diabetes_en.pdf)
- [2] *WHO News-Fact Sheets Diabetes Mellitus*. Accessed: Feb. 12, 2018. [Online]. Available: <http://www.who.int/mediacentre/factsheets/fs312/en/>
- [3] M. Righettoni and A. Tricoli, "Toward portable breath acetone analysis for diabetes detection," *J. Breath Res.*, vol. 5, no. 3, p. 037109, 2011.
- [4] P. Songthung and K. Sripanidkulchai, "Improving type 2 diabetes mellitus risk prediction using classification," in *Proc. 13th Int. Joint Conf. Comput. Sci. Softw. Eng. (JCSSE)*, 2016, pp. 1–6.
- [5] B. Bhowmik, V. Manjuladevi, R. K. Gupta, and P. Bhattacharyya, "Highly selective low-temperature acetone sensor based on hierarchical 3-D TiO<sub>2</sub> nanoflowers," *IEEE Sensors J.*, vol. 16, no. 10, pp. 3488–3495, May 2016.
- [6] S. Das, A. Bag, R. Kumar, and D. Biswas, "Fast response (7.6s) acetone sensing by InGa<sub>0.5</sub>N<sub>0.5</sub>/Ga<sub>0.5</sub>N on Si (111) at 373 K," *IEEE Electron Device Lett.*, vol. 38, no. 3, pp. 383–386, Mar. 2017.
- [7] A. Rydosz, K. Wincza, and S. Gruszczynski, "Microsystem in LTCC technology for the detection of acetone in healthy and diabetes breath," in *Proc. IEEE Andescon*, Oct. 2016, pp. 1–4.
- [8] Z. Y. Gong et al., "A ringdown breath acetone analyzer: Performance and validation using gas chromatography-mass spectrometry," *J. Anal. Bioanal. Technol.*, 2015. [Online]. Available: [www.omicsonline.org/open-access/a-ringdown-breath-acetone-analyzer-2155-9872.S7-013.php?aid=28338](http://www.omicsonline.org/open-access/a-ringdown-breath-acetone-analyzer-2155-9872.S7-013.php?aid=28338), doi: 10.4172/2155-9872.S7-013.
- [9] A. Nooke, "Gas detection by means of surface plasmon resonance enhanced ellipsometry," Bundesanstalt für Materialforschung und -prüfung (BAM), Berlin, Germany, Tech. Rep. Band 89, 2012.
- [10] B. Lakard, S. Carquigny, O. Segut, T. Patois, and S. Lakard, "Gas sensors based on electrodeposited polymers," *Metals*, vol. 5, no. 3, pp. 1371–1386, 2015.
- [11] S. Karthikeyan, H. M. Pandya, M. U. Sharma, and K. Gopal, "Gas sensors—A review," *J. Environ. Nanotechnol.*, vol. 4, no. 4, pp. 1–14, 2015.
- [12] Z. Jiang et al., "Highly sensitive acetone sensor based on Eu-doped SnO<sub>2</sub> electrospun nanofibers," *Ceram. Int.*, vol. 42, no. 14, pp. 15881–15888, 2016.
- [13] T. Hyodo, T. Kaino, T. Ueda, K. Izawa, and Y. Shimizu, "Acetone-sensing properties of WO<sub>3</sub>-based gas sensors operated in dynamic temperature modulation mode—Effects of loading of noble metal and/or NiO onto WO<sub>3</sub>," *Sensors Mater.*, vol. 28, no. 11, pp. 1179–1189, 2016.
- [14] G. W. Hunter, R. A. Dweik, D. B. Makel, C. C. Grigsby, R. S. Mayes, and C. E. Davis, "Portable breath monitoring: A new frontier in personalized health care," *Electrochem. Soc. Interface*, vol. 25, no. 4, pp. 63–67, 2016.
- [15] K. Toda, R. Furue, and S. Hayami, "Recent progress in applications of graphene oxide for gas sensing: A review," *Anal. Chim. Acta*, vol. 878, pp. 43–53, Jun. 2015.
- [16] J. Lou, Y. Wang, and L. Tong, "Microfiber optical sensors: A review," *Sensors*, vol. 14, no. 4, pp. 5823–5844, 2014.
- [17] D. R. Thévenot, K. Toth, R. A. Durst, and G. S. Wilson, "Electrochemical biosensors: Recommended definitions and classification," *Pure Appl. Chem.*, vol. 71, no. 12, pp. 2333–2348, 1999.
- [18] *Biocore Assay Handbook, 29-0194-00 Edition AA*, Bio-Sci. AB, Uppsala, Sweden, 2012, p. 5.
- [19] V. Perumal and U. Hashim, "Advances in biosensors: Principle, architecture and applications," *J. Appl. Biomed.*, vol. 12, no. 1, pp. 1–15, 2014.

- [20] S. Malhotra, A. Verma, N. Tyagi, and V. Kumar, "BioSensors: Principle, types and applications," *Int. J. Adv. Res. Innov. Ideas Educ.*, vol. 3, no. 2, pp. 3639–3644, 2017.
- [21] E. Bakker and M. Telting-Diaz, "Electrochemical sensors," *Anal. Chem.*, vol. 74, no. 12, pp. 2781–2800, 2002.
- [22] B. R. Eggins, *Chemical Sensors and Biosensors* vol. 28. Hoboken, NJ, USA: Wiley, 2008.
- [23] D. Dey and T. Goswami, "Optical biosensors: A revolution towards quantum nanoscale electronics device fabrication," *J. Biomed. Biotechnol.*, vol. 2011, 2011, Art. no. 348218.
- [24] D. R. Thévenot, K. Toth, R. A. Durst, and G. S. Wilson, "Electrochemical biosensors: Recommended definitions and classification," *Biosensors Bioelectron.*, vol. 34, no. 5, pp. 635–659, 2001.
- [25] M. S. Ünlü, M. Chiari, and A. Özcan, "Introduction to the special issue of optical biosensors," *Nanophotonics*, vol. 6, no. 4, pp. 623–625, 2017.
- [26] S. M. Borisov and O. S. Wolfbeis, "Optical biosensors," *Chem. Rev.*, vol. 108, no. 2, pp. 423–461, 2008.
- [27] Y.-S. Sun, J. P. Landry, and X. D. Zhu, "Evaluation of kinetics using label-free optical biosensors," *Instrum. Sci. Technol.*, vol. 45, no. 5, pp. 486–505, 2017.
- [28] F. S. Ligler and C. R. Taitt, *Optical Biosensors: Present & Future*. Houston, TX, USA: Gulf Professional Publishing, 2002.
- [29] K. Staszek, A. Rydosz, E. Maciak, K. Wincza, and S. Gruszczynski, "Six-port microwave system for volatile organic compounds detection," *Sens. Actuators B, Chem.*, vol. 245, pp. 882–894, Jun. 2017.
- [30] H. Torun, F. C. Top, G. Dundar, and A. D. Yalcinkaya, "An antenna-coupled split-ring resonator for biosensing," *J. Appl. Phys.*, vol. 116, no. 12, p. 124701, 2014.
- [31] B. Camli, E. Kusakci, B. Lafci, S. Salman, H. Torun, and A. Yalcinkaya, "A microwave ring resonator based glucose sensor," *Procedia Eng.*, vol. 168, pp. 465–468, Jan. 2016.
- [32] M. Righettoni, A. Tricoli, S. Gass, A. Schmid, A. Amann, and S. E. Pratsinis, "Breath acetone monitoring by portable Si:WO<sub>3</sub> gas sensors," *Anal. Chim. Acta*, vol. 738, pp. 69–75, Aug. 2012.
- [33] C.-M. Yang, T.-C. Chen, Y.-C. Yang, M.-C. Hsiao, M. Meyyappan, and C.-S. Lai, "Ultraviolet illumination effect on monolayer graphene-based resistive sensor for acetone detection," *Vacuum*, vol. 140, pp. 89–95, Jun. 2017.
- [34] S. M. Hicks and A. J. Killard, "Electrochemical impedance characterisation of tungsten trioxide–polyaniline nanocomposites for room temperature acetone sensing," *Sens. Actuators B, Chem.*, vol. 194, pp. 283–289, Apr. 2014.
- [35] Q. Zhang and D. Wang, "Room temperature acetone sensor based on nanostructured K<sub>2</sub>W<sub>7</sub>O<sub>22</sub>," in *Proc. IEEE SENSORS*, Oct./Nov. 2016, pp. 1–3.
- [36] R. F. Taylor and J. S. Schultz, *Handbook of Chemical and Biological Sensors*. Boca Raton, FL, USA: CRC Press, 1996.
- [37] J. L. Santos and F. Farahi, *Handbook of Optical Sensors*. Boca Raton, FL, USA: CRC Press, 2014.
- [38] H. Bai and G. Shi, "Gas sensors based on conducting polymers," *Sensors*, vol. 7, no. 3, pp. 267–307, 2007.
- [39] I. Fratoddi, I. Venditti, C. Cametti, and M. V. Russo, "Chemiresistive polyaniline-based gas sensors: A mini review," *Sens. Actuators B, Chem.*, vol. 220, pp. 534–548, Dec. 2015.
- [40] N. Ramgir et al., "Metal oxide nanowires for chemiresistive gas sensors: Issues, challenges and prospects," *Colloids Surfaces A, Physicochem. Eng. Aspects*, vol. 439, pp. 101–116, Dec. 2013.
- [41] V. K. Tomer, K. Singh, H. Kaur, M. Shorie, and P. Sabherwal, "Rapid acetone detection using indium loaded WO<sub>3</sub>/SnO<sub>2</sub> nanohybrid sensor," *Sens. Actuators B, Chem.*, vol. 253, pp. 703–713, Dec. 2017.
- [42] T. Xiao et al., "Highly sensitive and selective acetone sensor based on C-doped WO<sub>3</sub> for potential diagnosis of diabetes mellitus," *Sens. Actuators B, Chem.*, vol. 199, pp. 210–219, Aug. 2014.
- [43] M. Yin, L. Yu, and S. Liu, "Synthesis of thickness-controlled cuboid WO<sub>3</sub> nanosheets and their exposed facets-dependent acetone sensing properties," *J. Alloys Compounds*, vol. 696, pp. 490–497, Nov. 2017.
- [44] J.-Y. Shen, L. Zhang, J. Ren, J.-C. Wang, H.-C. Yao, and Z.-J. Li, "Highly enhanced acetone sensing performance of porous C-doped WO<sub>3</sub> hollow spheres by carbon spheres as templates," *Sens. Actuators B, Chem.*, vol. 239, pp. 597–607, Feb. 2017.
- [45] H. Jamalabadi and N. Alizadeh, "Enhanced low-temperature response of PPy-WO<sub>3</sub> hybrid nanocomposite based gas sensor deposited by electrospinning method for selective and sensitive acetone detection," *IEEE Sensors J.*, vol. 17, no. 8, pp. 2322–2328, Apr. 2017.
- [46] S. Salehi, E. Nikan, A. A. Khodadadi, and Y. Mortazavi, "Highly sensitive carbon nanotubes–SnO<sub>2</sub> nanocomposite sensor for acetone detection in diabetes mellitus breath," *Sens. Actuators B, Chem.*, vol. 205, pp. 261–267, Dec. 2014.
- [47] J. Luo et al., "Nanoparticle-structured thin film sensor arrays for breath sensing," *Sens. Actuators B, Chem.*, vol. 161, pp. 845–854, Jan. 2012.
- [48] J.-B. Yu, H.-G. Byun, M.-S. So, and J.-S. Huh, "Analysis of diabetic patient's breath with conducting polymer sensor array," *Sens. Actuators B, Chem.*, vol. 108, pp. 305–308, Jul. 2005.
- [49] T. I. Nasution, I. Nainggolan, S. D. Hutagalung, K. R. Ahmad, and Z. A. Ahmad, "The sensing mechanism and detection of low concentration acetone using chitosan-based sensors," *Sens. Actuators B, Chem.*, vol. 177, pp. 522–528, Feb. 2013.
- [50] S. Wei, G. Zhao, W. Du, and Q. Tian, "Synthesis and excellent acetone sensing properties of porous WO<sub>3</sub> nanofibers," *Vacuum*, vol. 124, pp. 32–39, Feb. 2016.
- [51] S. Kundu, I. Subramanian, M. Narjinary, and R. Manna, "Enhanced performance of  $\gamma$ -Fe<sub>2</sub>O<sub>3</sub>: WO<sub>3</sub> nanocomposite towards selective acetone vapor detection," *Ceram. Int.*, vol. 42, no. 6, pp. 7309–7314, 2016.
- [52] M. Narjinary, P. Rana, A. Sen, and M. Pal, "Enhanced and selective acetone sensing properties of SnO<sub>2</sub>-MWCNT nanocomposites: Promising materials for diabetes sensor," *Mater. Des.*, vol. 115, pp. 158–164, Feb. 2017.
- [53] Y. Zhang et al., "Gas sensor based on samarium oxide loaded mulberry-shaped tin oxide for highly selective and sub ppm-level acetone detection," *J. Colloid Interface Sci.*, vol. 531, pp. 74–82, Dec. 2018.
- [54] H. G. Moon et al., "Hollow Pt-functionalized SnO<sub>2</sub> hemipill network formation using a bacterial skeleton for the noninvasive diagnosis of diabetes," *ACS Sensors*, vol. 3, no. 3, pp. 661–669, 2018.
- [55] Z. Liu et al., "Enhanced selective acetone sensing characteristics based on Co-doped WO<sub>3</sub> hierarchical flower-like nanostructures assembled with nanoplates," *Sens. Actuators B, Chem.*, vol. 235, pp. 614–621, Nov. 2016.
- [56] J. Shi et al., "WO<sub>3</sub> nanocrystals: Synthesis and application in highly sensitive detection of acetone," *Sens. Actuators B, Chem.*, vol. 156, pp. 820–824, Aug. 2011.
- [57] M. Esmaili, G. Kiani, F. S. Nogorani, and S. Boroomand, "Acetone sensing properties of hierarchical WO<sub>3</sub> core-shell microspheres in comparison with commercial nanoparticles," *Int. J. Nano Dimension*, vol. 7, no. 3, pp. 254–262, 2016.
- [58] N.-H. Kim et al., "Highly sensitive and selective acetone sensing performance of WO<sub>3</sub> nanofibers functionalized by Rh<sub>2</sub>O<sub>3</sub> nanoparticles," *Sens. Actuators B, Chem.*, vol. 224, pp. 185–192, Mar. 2016.
- [59] A. Rydosz, A. Szkudlarek, M. Ziabka, K. Domanski, W. Maziarz, and T. Pisarkiewicz, "Performance of Si-doped WO<sub>3</sub> thin films for acetone sensing prepared by glancing angle DC magnetron sputtering," *IEEE Sensors J.*, vol. 16, no. 4, pp. 1004–1012, Feb. 2016.
- [60] X. Zhang, Z. Dong, S. Liu, Y. Shi, Y. Dong, and W. Feng, "Maize straw-templated hierarchical porous ZnO:Ni with enhanced acetone gas sensing properties," *Sens. Actuators B, Chem.*, vol. 243, pp. 1224–1230, May 2017.
- [61] A. J. Kulandaisamy, V. Elavallagan, P. Shankar, G. K. Mani, K. J. Babu, and J. B. B. Rayappan, "Nanostructured Cerium-doped ZnO thin film—A breath sensor," *Ceram. Int.*, vol. 42, pp. 18289–18295, Dec. 2016.
- [62] F. Liu et al., "High performance mixed potential type acetone sensor based on stabilized zirconia and NiNb<sub>2</sub>O<sub>6</sub> sensing electrode," *Sens. Actuators B, Chem.*, vol. 229, pp. 200–208, Jun. 2016.
- [63] S. Park, "Acetone gas detection using TiO<sub>2</sub> nanoparticles functionalized In<sub>2</sub>O<sub>3</sub> nanowires for diagnosis of diabetes," *J. Alloys Compounds*, vol. 696, pp. 655–662, Nov. 2017.
- [64] P. Wang et al., "Superior acetone sensor based on single-crystalline  $\alpha$ -Fe<sub>2</sub>O<sub>3</sub> mesoporous nanospheres via [C<sub>12</sub>mim][BF<sub>4</sub>]-assistant synthesis," *Sens. Actuators B, Chem.*, vol. 241, pp. 967–977, Mar. 2017.
- [65] C.-M. Yang, T.-C. Chen, Y.-C. Yang, M. Meyyappan, and C.-S. Lai, "Enhanced acetone sensing properties of monolayer graphene at room temperature by electrode spacing effect and UV illumination," *Sens. Actuators B, Chem.*, vol. 253, pp. 77–84, Dec. 2017.
- [66] X. Hao et al., "Mixed potential type sensor based on stabilized zirconia and Co<sub>1-x</sub>Zn<sub>x</sub>Fe<sub>2</sub>O<sub>4</sub> sensing electrode for detection of acetone," *Sens. Actuators B, Chem.*, vol. 255, pp. 1173–1181, Feb. 2017.
- [67] X. Liang et al., "Synthesis of In<sub>2</sub>O<sub>3</sub> hollow nanofibers and their application in highly sensitive detection of acetone," *Ceram. Int.*, vol. 41, no. 10, pp. 13780–13787, 2015.

- [68] J. Li, L. Wang, Z. Liu, Y. Wang, and S. Wang, "Au-modified  $\alpha$ -Fe<sub>2</sub>O<sub>3</sub> columnar superstructures assembled with nanoplates and their highly improved acetone sensing properties," *J. Alloys Compounds*, vol. 728, pp. 944–951, Dec. 2017.
- [69] R. C. Pullar et al., "Pt-decorated In<sub>2</sub>O<sub>3</sub> nanoparticles and their ability as a highly sensitive (<10 ppb) acetone sensor for biomedical applications," *Sens. Actuators B, Chem.*, vol. 230, pp. 697–705, Mar. 2016.
- [70] A. Fioravanti, S. Morandi, and M. C. Carotta, "Chemoresistive gas sensors for sub-ppm acetone detection," in *Proc. 30th Eurosensors Conf.*, vol. 168, 2016, pp. 485–488.
- [71] Y. Xie, R. Xing, Q. Li, L. Xu, and H. Song, "Three-dimensional ordered ZnO–CuO inverse opals toward low concentration acetone detection for exhaled breath sensing," *Sens. Actuators B, Chem.*, vol. 211, pp. 255–262, May 2015.
- [72] R. C. Biswal, "Pure and Pt-loaded gamma iron oxide as sensor for detection of sub ppm level of acetone," *Sens. Actuators B, Chem.*, vol. 157, pp. 183–188, Sep. 2011.
- [73] B. Bhowmik, K. Dutta, A. Hazra, and P. Bhattacharyya, "Low temperature acetone detection by p-type nano-titania thin film: Equivalent circuit model and sensing mechanism," *Solid-State Electron.*, vol. 99, pp. 84–92, Sep. 2014.
- [74] F. Liu et al., "Highly sensitive gas sensor based on stabilized zirconia and CdMoO<sub>4</sub> sensing electrode for detection of acetone," *Sens. Actuators B, Chem.*, vol. 248, pp. 9–18, Sep. 2017.
- [75] P. Zhang, H. Qin, W. Lv, H. Zhang, and J. Hu, "Gas sensors based on ytterbium ferrites nanocrystalline powders for detecting acetone with low concentrations," *Sens. Actuators B, Chem.*, vol. 246, pp. 9–19, Jul. 2017.
- [76] J. Hu et al., "One-step synthesis of 2D C<sub>3</sub>N<sub>4</sub>-tin oxide gas sensors for enhanced acetone vapor detection," *Sens. Actuators B, Chem.*, vol. 253, pp. 641–651, Dec. 2017.
- [77] C. Wang et al., "Ultrasensitive and low detection limit of acetone gas sensor based on W-doped NiO hierarchical nanostructure," *Sens. Actuators B, Chem.*, vol. 220, pp. 59–67, Dec. 2015.
- [78] W. Xiaofeng et al., "Sensing performances to low concentration acetone for palladium doped LaFeO<sub>3</sub> sensors," *J. Rare Earths*, vol. 34, pp. 704–710, Jul. 2016.
- [79] Q. Zhang, P. Wang, J. Li, and X. Gao, "Diagnosis of diabetes by image detection of breath using gas-sensitive lps," *Biosensors Bioelectron.*, vol. 15, nos. 5–6, pp. 249–256, 2000.
- [80] K. Pramanik, P. Sarkar, and D. Bhattacharyya, "Estimation of acetone in breath using  $\alpha$ -D-galactose for diabetes monitoring," *Int. J. Eng. Innov. Technol.*, vol. 4, no. 8, pp. 119–123, 2015.
- [81] L. Zhang et al., "Three-dimensional ordered ZnO–Fe<sub>3</sub>O<sub>4</sub> inverse opal gas sensor toward trace concentration acetone detection," *Sens. Actuators B, Chem.*, vol. 252, pp. 367–374, Nov. 2017.
- [82] K. Muthukrishnan et al., "Studies on acetone sensing characteristics of ZnO thin film prepared by sol–gel dip coating," *J. Alloys Compounds*, vol. 673, pp. 138–143, Jul. 2016.
- [83] C. Liu et al., "Acetone gas sensor based on NiO/ZnO hollow spheres: Fast response and recovery, and low (ppb) detection limit," *J. Colloid Interface Sci.*, vol. 495, pp. 207–215, Jun. 2017.
- [84] W. Liu et al., "A highly sensitive and moisture-resistant gas sensor for diabetes diagnosis with Pt@In<sub>2</sub>O<sub>3</sub> nanowires and a molecular sieve for protection," *NPG Asia Mater.*, p. 1, 2018.
- [85] L. F. Da Silva et al., "Acetone gas sensor based on  $\alpha$ -Ag<sub>2</sub>WO<sub>4</sub> nanorods obtained via a microwave-assisted hydrothermal route," *J. Alloys Compounds*, vol. 683, pp. 186–190, Oct. 2016.
- [86] W.-T. Koo, S.-J. Choi, J.-S. Jang, and I.-D. Kim, "Metal-organic framework templated synthesis of ultrasmall catalyst loaded ZnO/ZnCo<sub>2</sub>O<sub>4</sub> hollow spheres for enhanced gas sensing properties," *Sci. Rep.*, vol. 7, Mar. 2017, Art. no. 45074.
- [87] C. Liu et al., "Facile synthesis and the enhanced sensing properties of Pt-loaded  $\alpha$ -Fe<sub>2</sub>O<sub>3</sub> porous nanospheres," *Sens. Actuators B, Chem.*, vol. 252, pp. 1153–1162, Nov. 2017.
- [88] F. Liu et al., "Sub-ppm YSZ-based mixed potential type acetone sensor utilizing columbite type composite oxide sensing electrode," *Sens. Actuators B, Chem.*, vol. 238, pp. 928–937, Jan. 2017.
- [89] T. L. Porter, M. P. Eastman, D. L. Pace, and M. Bradley, "Sensor based on piezoresistive microcantilever technology," *Sens. Actuators A, Phys.*, vol. 88, pp. 47–51, Jan. 2001.
- [90] C. W. Hanson and E. R. Thaler, "Electronic nose prediction of a clinical pneumonia score: Biosensors and microbes," *Anesthesiol., J. Amer. Soc. Anesthesiol.*, vol. 102, no. 1, pp. 63–68, 2005.
- [91] M. Ye, P.-J. Chien, K. Toma, T. Arakawa, and K. Mitsubayashi, "An acetone bio-sniffer (gas phase biosensor) enabling assessment of lipid metabolism from exhaled breath," *Biosensors Bioelectron.*, vol. 73, pp. 208–213, Nov. 2015.
- [92] A. D. Worrall, J. A. Bernstein, and A. P. Angelopoulos, "Portable method of measuring gaseous acetone concentrations," *Talanta*, vol. 112, pp. 26–30, Aug. 2013.
- [93] C. L. Wong, U. S. Dinis, M. S. Schmidt, and M. Olivo, "Non-labeling multiplex surface enhanced Raman scattering (SERS) detection of volatile organic compounds (VOCs)," *Anal. Chim. Acta*, vol. 844, pp. 54–60, Sep. 2014.
- [94] T. P. J. Blaikie et al., "Portable device for measuring breath acetone based on sample preconcentration and cavity enhanced spectroscopy," *Anal. Chem.*, vol. 88, no. 22, pp. 11016–11021, 2016.
- [95] A. A. Alwahib et al., "Reduced graphene oxide/maghemite nanocomposite for detection of hydrocarbon vapor using surface plasmon resonance," *IEEE Photon. J.*, vol. 8, no. 4, Aug. 2016, Art. no. 4802009.
- [96] P. Gunawan et al., "Ultrahigh sensitivity of Au/ID  $\alpha$ -Fe<sub>2</sub>O<sub>3</sub> to acetone and the sensing mechanism," *Langmuir*, vol. 28, no. 39, pp. 14090–14099, 2012.
- [97] A. Rydosz, E. Maciak, K. Wincza, and S. Gruszczynski, "Microwave-based sensors with phthalocyanine films for acetone, ethanol and methanol detection," *Sens. Actuators B, Chem.*, vol. 237, pp. 876–886, Jul. 2016.
- [98] D. Fu et al., "Polymer coated silicon microring device for the detection of sub-ppm volatile organic compounds," *Sens. Actuators B, Chem.*, vol. 257, pp. 136–142, Mar. 2018.
- [99] Z. Y. Li, G. Zhang, Z. C. Yang, Y. L. Hao, Y. F. Jin, and A. Q. Liu, "Highly sensitive and integrated VOC sensor based on silicon nanophotonics," in *Proc. 19th Int. Conf. Solid-State Sensors, Actuators, Microsyst. (TRANSDUCERS)*, 2017, pp. 1479–1482.
- [100] S. Rauf, Y. Ali, S. Hussain, F. Ullah, and A. Hayat, "Design of a novel filter paper based construct for rapid analysis of acetone," *PLoS ONE*, vol. 13, no. 7, p. e0199978, 2018.
- [101] M. A. Suster and P. Mohseni, "An RF/microwave microfluidic sensor based on a center-gapped microstrip line for miniaturized dielectric spectroscopy," in *IEEE MTT-S Int. Microw. Symp. Dig.*, Jun. 2013, pp. 1–3.
- [102] A. Sohrabi, P. M. Shaibani, M. H. Zarifi, M. Daneshmand, and T. Thundat, "A novel technique for rapid vapor detection using swelling polymer covered microstrip ring resonator," in *IEEE MTT-S Int. Microw. Symp. Dig.*, Jun. 2014, pp. 1–4.
- [103] M. H. Zarifi, A. Sohrabi, P. M. Shaibani, M. Daneshmand, and T. Thundat, "Detection of volatile organic compounds using microwave sensors," *IEEE Sensors J.*, vol. 15, no. 1, pp. 248–254, Jan. 2015.
- [104] I. Osica et al., "Highly networked capsular silica–porphyrin hybrid nanostructures as efficient materials for acetone vapor sensing," *ACS Appl. Mater. Interfaces*, vol. 9, no. 11, pp. 9945–9954, 2017.
- [105] A. Hulanicki, S. Glab, and F. Ingman, "Chemical sensors: Definitions and classification," *Pure Appl. Chem.*, vol. 63, no. 9, pp. 1247–1250, 1991.
- [106] J. O. Dennis, A. A. S. Rabih, M. H. M. Khir, M. G. A. Ahmed, and A. Y. Ahmed, "Modeling and finite element analysis simulation of MEMS based acetone vapor sensor for noninvasive screening of diabetes," *J. Sensors*, vol. 2016, Apr. 2016, Art. no. 9563938.
- [107] W. Tao, P. Lin, S. Liu, Q. Xie, S. Ke, and X. Zeng, "1-butyl-3-methylimidazolium tetrafluoroborate film as a highly selective sensing material for non-invasive detection of acetone using a quartz crystal microbalance," *Sensors*, vol. 17, p. 194, Jan. 2017.
- [108] Z. Ying, Y. Jiang, X. Du, G. Xie, J. Yu, and H. Wang, "PVDF coated quartz crystal microbalance sensor for DMMP vapor detection," *Sens. Actuators B, Chem.*, vol. 125, no. 1, pp. 167–172, 2007.
- [109] M. M. Ayad, N. Salahuddin, and I. M. Minisy, "Detection of some volatile organic compounds with chitosan-coated quartz crystal microbalance," *Designed Monomers Polymers*, vol. 17, no. 8, pp. 795–802, 2014.
- [110] H.-Y. Li, T.-H. Hsu, C.-Y. Chen, M.-C. Tseng, and Y.-H. Chu, "Exploring silver ionic liquids for reaction-based gas sensing on a quartz crystal microbalance," *Analyst*, vol. 140, no. 18, pp. 6245–6249, 2015.
- [111] A. Daneshkhah, S. Shrestha, M. Agarwal, and K. Varahramyan, "PPy/PMMA/PEG-based sensor for low-concentration acetone detection," *Proc. SPIE*, vol. 9107, p. 910712, May 2014.
- [112] A. K. M. S. Islam et al., "Transient parameters of a coated quartz crystal microbalance sensor for the detection of volatile organic compounds (VOCs)," *Sens. Actuators B, Chem.*, vol. 109, no. 2, pp. 238–243, 2005.

- [113] S. Zhang, Z. K. Chen, G. W. Bao, and S. F. Y. Li, "Organic vapor detection by quartz crystal microbalance modified with mixed multilayer Langmuir-Blodgett films," *Talanta*, vol. 45, pp. 727–733, Feb. 1998.
- [114] Z. Ying, Y. Jiang, H. Qin, L. Zheng, and X. Du, "A study on QCM sensor for identification of acetone vapor," *COMPEL-Int. J. Comput. Math. Elect. Electron. Eng.*, vol. 29, no. 2, pp. 477–483, 2010.
- [115] M. Frank, T. T. Nguyen, F. M. Makau, K. S. Moon, and S. Kassegne, "PMN-PT single crystal resonators for sensing acetone vapors," *Proc. SPIE*, vol. 7266, p. 72660U, Nov. 2008.
- [116] X. Xu, H. Cang, C. Li, Z. K. Zhao, and H. Li, "Quartz crystal microbalance sensor array for the detection of volatile organic compounds," *Talanta*, vol. 78, pp. 711–716, May 2009.
- [117] K.-H. Kim, S. A. Jahan, and E. Kabir, "A review of breath analysis for diagnosis of human health," *TrAC Trends Anal. Chem.*, vol. 33, pp. 1–8, Mar. 2012.
- [118] D. Zhang, D. Guo, and K. Yan, *Breath Analysis for Medical Applications*. Cham, Switzerland: Springer, 2017.
- [119] W. Tao, P. Lin, Y. Ai, H. Wang, S. Ke, and X. Zeng, "Multichannel quartz crystal microbalance array: Fabrication, evaluation, application in biomarker detection," *Anal. Biochem.*, vol. 494, pp. 85–92, Feb. 2016.
- [120] H. Huang, J. Zhou, S. Chen, L. Zeng, and Y. Huang, "A highly sensitive QCM sensor coated with Ag<sup>+</sup>-ZSM-5 film for medical diagnosis," *Sens. Actuators B, Chem.*, vol. 101, pp. 316–321, Jul. 2004.
- [121] S. K. Vashist and P. Vashist, "Recent advances in quartz crystal microbalance-based sensors," *J. Sensors*, vol. 2011, Jun. 2011, Art. no. 571405.
- [122] K. Zhang, R. Hu, G. Fan, and G. Li, "Graphene oxide/chitosan nanocomposite coated quartz crystal microbalance sensor for detection of amine vapors," *Sens. Actuators B, Chem.*, vol. 243, pp. 721–730, May 2017.
- [123] J. O. Dennis, A. A. S. Rabih, M. H. M. Khir, M. G. A. Ahmed, and A. Y. Ahmed, "Modeling and finite element analysis simulation of MEMS based acetone vapor sensor for noninvasive screening of diabetes," *J. Sensors*, vol. 2016, Apr. 2016, Art. no. 9563938.
- [124] A. A. S. Rabih et al., "MEMS-based acetone vapor sensor for non-invasive screening of diabetes," *IEEE Sensors J.*, vol. 18, no. 23, pp. 9486–9500, Dec. 2018.
- [125] J. Chen, X. Pan, F. Boussaid, A. Bermak, and Z. Fan, "A hierarchical ZnO nanostructure gas sensor for human breath-level acetone detection," in *Proc. IEEE Int. Symp. Circuits Syst. (ISCAS)*, May 2016, pp. 1866–1869.



**A. Y. AHMED** (M'08) was born in Wad Madani, Sudan in 1980. He received the B.Sc. degree (Hons.) in electronic engineering from the University of Gezira, Wad Medani, Sudan, in 2006, and the M.Sc. and Ph.D. degrees in electrical and electronics engineering from Universiti Teknologi PETRONAS, Malaysia, in 2009 and 2015, respectively. In 2016, he joined Universiti Teknologi PETRONAS, where he is currently a Lecturer with the Electrical and Electronic Engineering Department. His area of focus is microelectromechanical systems actuator/sensor design and microfabrication/sensor technology based on CMOS-MEMS technologies.



**FABRICE MERIAUDEAU** was born in Villeurbanne, France, in 1971. He received both the Engineering degree in material sciences and master's degree in physics and the Ph.D. degree in image processing from Dijon University, France, in 1994 and 1997, respectively. He held a Post-doctoral position at the Oak Ridge National Laboratory for a year. He has coordinated an Erasmus Mundus Master in the field of computer vision and robotics, from 2006 to 2010. From 2010 to 2012, he was the Vice President for International Affairs of the University of Burgundy, where he is currently the Professeur des Universités. He was the Director of the Le2i, UMR CNRS, which has more than 200 staff members, from 2011 to 2016. In 2016, he joined Universiti Teknologi PETRONAS as a Full Professor and was appointed as the Director of the Institute Health and Analytics, in 2017. In 2018, he returned to the University of Burgundy. He has authored or co-authored more than 150 international publications and holds several patents. His research interests are focused on image processing for non-conventional imaging systems (UV, IR, polarization, and so on) and more recently on medical/biomedical imaging.



**O. B. AYODELE** received the bachelor's degree in chemical engineering from the Federal University of Technology Minna, Nigeria, the M.Sc. degree (research mode) in heterogeneous catalysis for wastewater treatment from the University of Science Malaysia (USM), and the Ph.D. degree in renewable energy from the University of Malaya, Malaysia. His Post-doctoral study as a Research Scientist (RS) was funded by the Mitsubishi Corporation Education Trust Fund, Center for Biofuel and Biochemical Research, Universiti Teknologi PETRONAS, Malaysia. He was a Visiting RS with the Clean Energy Research Center, University of Yamanashi, Kofu, Japan. After his Post-doctoral study, he was appointed as a Senior Lecturer at the Department of Chemical Engineering, Universiti Teknologi PETRONAS. He is currently a Research Fellow with the International Iberian Nanotechnology Laboratory, Braga, Portugal. His recent findings in the field of catalysis and energy were published as a sole author article by *Scientific Reports Nature*. During his M.Sc. degree, he received two prestigious USM Hall of Fame Awards of Excellence in Research and Publication. He received the University of Malaya Award of Excellence for completing his Ph.D. degree in less than three years. He serves as an Associate Editor for the *Malaysian Journal of Catalysis* and as an Editorial Board Member of the *Open Materials Science Journal*.



**ALMUR A. S. RABIH** (M'09) was born in Wad Madani, Sudan in 1983. He received the B.Sc. degree (Hons.) in electronic engineering (specialization in medical instrumentation) from the University of Gezira, Wad Medani, Sudan, 2008, and the M.Sc. and Ph.D. degrees in electrical and electronic engineering from Universiti Teknologi PETRONAS, Malaysia, in 2012 and 2018, respectively. He then joined the University of Gezira, as a Teaching Assistant, where he is currently an Assistant Professor with the Faculty of Engineering and Technology. His area of focus is Bio-MEMS, medical devices, and breath analysis.



**FAHAD USMAN** was born in Kankara-Katsina, Nigeria in 1987. He received the B.Sc. degree (Hons.) in physics from the Usmanu Danfodiyo University, Sokoto, Nigeria, in 2012, and the M.Sc. degree in medical physics from Universiti Sains Malaysia, in 2015. He is currently pursuing the Ph.D. degree in applied physics (medical biosensors) with Universiti Teknologi PETRONAS, Malaysia. Since 2016, he has been a Physics Lecturer with Al-Qalam University, Katsina, Nigeria. His area of focus is mainly in the application of physics in medicine that includes areas, such as medical imaging, medical devices, radiation physics, and breathe analysis.



**J. O. DENNIS** (SM'16) was born in Malakal, South Sudan in 1959. He received the Bachelor of Education (Science) degree in mathematics and physics from the University of Juba, Juba, South Sudan, in 1982, and the Ph.D. degree in applied physics from Universiti Teknologi Malaysia, Malaysia, in 2001. In 2003, he joined the Electrical and Electronic Engineering Department, Universiti Teknologi PETRONAS, as a Senior Lecturer. He is currently an Associate Professor with the Department of Fundamental and Applied Sciences, Universiti Teknologi PETRONAS. His current focus of research is in microelectromechanical systems design, simulation, and fabrication.